Photoionization and photofragmentation of the C_{60}^{+} molecular ion

K. K. Baral, N. B. Aryal, D. A. Esteves-Macaluso, C. M. Thomas, J. Hellhund, R. Lomsadze,
A. L. D. Kilcoyne, A. Müller, S. Schippers, and R. A. Phaneuf

Photoionization and photofragmentation of the C$_{60}^+$ molecular ion

K. K. Baral,[1] N. B. Aryal,[1] D. A. Esteves-Macaluso,[1, *] C. M. Thomas,[1] J. Hellhund,[2, 1]
R. Lomsadze,[1, †] A. L. D. Kilcoyne,[3] A. Müller,[2] S. Schippers,[2, 4] and R. A. Phaneuf[1, ‡]

[1]*Department of Physics, University of Nevada, Reno, Nevada 89557-0220*
[2]*Institut für Atom- und Molekülphysik, Justus-Liebig-Universität-Giessen, D-35392 Giessen, Germany*
[3]*Advanced Light Source, MS 7-100, Lawrence Berkeley National Laboratory, Berkeley, CA 94720*
[4]*I. Physikalisches Institut, Justus-Liebig-Universität-Giessen, 35392 Giessen, Germany*

Cross-section measurements are reported for single and double photoionization of C$_{60}^+$ ions in the photon energy range 18–150 eV accompanied by the loss of zero to seven pairs of carbon atoms, as well as for fragmentation without ionization resulting in loss of two to eight pairs of C atoms in the photon energy range 18–65 eV. Absolute measurements were performed by merging a beam of C$_{60}^+$ molecular ions with a beam of monochromatized synchrotron radiation. Product channels involving dissocation yielding smaller fullerene fragment ions account for nearly half of the total measured oscillator strength in this energy range. The sum of cross sections for the measured product channels is compared to a published calculation of the total photoabsorption cross section of neutral C$_{60}$ based on time-dependent density-functional theory. This comparison and an accounting of oscillator strengths indicates that with the exception of C$_{58}^+$, the most important product channels resulting from photoabsorption were accounted for in the experiment. Threshold energies for the successive removal of carbon atom pairs accompanying photoionization are also determined from the measurements.

PACS numbers: 32.80.Fb, 32.70.Cs, 32.80.Aa
Keywords: fullerene, photoionization, fragmentation, absolute cross section, oscillator strength, threshold energy, synchrotron radiation, merged beams

I. INTRODUCTION

Fullerene molecules have been studied extensively since the Nobel Prize winning discovery of C$_{60}$ by Kroto and collaborators [1]. Their nanometer size, hollow cage structure, homonuclearity and high degree of symmetry give rise to novel properties that are intermediate between those of a free molecule and of a pure crystalline solid. The extensive body of research exploring the multiscale dynamics of photo-excited C$_{60}$ was recently reviewed by Lépine [2]. Measurements of photoionization of the C$_{60}$ molecule were first reported by Hertel et al. [3], who identified a broad resonance in the cross section near 20 eV that had been predicted theoretically [4] and attributed to a collective surface plasmon excitation of the 240 delocalized carbon valence electrons. These data were not on an absolute scale and were subsequently renormalized by Berkowitz [5] to the theoretical photoabsorption oscillator strength. Photoionization measurements for C$_{60}$ were subsequently reported by Yoo et al. [6] and Reinköster et al. [7]. More recently, measurements for single and multiple photoionization of C$_{60}$ in the 25–120 eV range were reported by Kafle and collaborators [8] who placed their results on an absolute scale

using revised data for the vapor pressure of C$_{60}$. Previously published data were revisited and the combined results compare favorably with theoretical data for total photoabsorption (60 times the cross section for a single C atom) and with the Thomas-Reiche-Kuhn (TRK) oscillator-strength sum rule [9].

Absolute photoionization cross-section measurements for fullerene ions were first reported by Scully et al. [10], who merged mass/charge analyzed ion beams with a beam of tuneable monochromatized synchrotron radiation. Cross sections for single photoionization of C$_{60}^+$, C$_{60}^{2+}$ and C$_{60}^{3+}$ ions were measured over the photon energy range 17–75 eV. In addition to the prominent surface plasmon resonance near 20 eV, a second broad feature was identified in the cross-section data near 40 eV that was attributed, on the basis of a theoretical calculation using the time-dependent local-density approximation, to a higher-order collective (volume) plasmon resonance [10–13].

Irradiation of fullerenes by energetic photons may also lead to the pairwise loss of C atoms. Their closed empty-cage geometries permit stable fullerene molecules C$_n$ to consist only of even numbers of C atoms with n $\geq$ 20, consistent with Euler's theorem for closed polyhedrons [13]. The first study of the dynamics of fragmentation of C$_{60}$ under energetic laser irradiation was reported by O'Brien et al. [14] using a time-of-flight technique. The loss of C$_2$ units was interpreted in terms of a "shrink-wrapping" mechanism in which a C$_{60}^+$ ion becomes unstable due to extensive vibrational excitation, and relaxes by ejecting one or more C$_2$ units to form a smaller fullerene molecule. Cross-section ratios for single, double and triple photoionization of C$_{60}$ accompanied by

the loss of up to 6 pairs of carbon atoms and their appearance potentials were reported by Juranic et al. [15]. Fragmentation of neutral C_{60} and C_{70} has been studied theoretically using a number of different approximations [16–22]. The C_2 fragmentation energies predicted by these calculations fall in the 10–12 eV range. Photoionization mass spectrometry measurements by Yoo et al. [6] on C_{60} determined the threshold energy for producing C_{58}^+ from C_{60}^+ to be in the range 6.0–6.5 eV, which is significantly lower than the theoretical predictions. Comparison of experimental results with theory is complicated by initial internal vibrational and rotational energy which have the effect of reducing the measured threshold energy for fragmentation.

Recently, absolute experimental cross sections for double photoionization of C_{60}^+ accompanied by the loss of as many as three carbon pairs were reported by Kilcoyne et al. [23] and Phaneuf et al. [24] in the photon energy range 60–150 eV as part of a study of photoelectron-wave interference effects in the endofullerene molecular ion $Xe@C_{60}^+$. This paper presents the results of a systematic experimental investigation of pure single and double photoionization as well as single and double photoionization accompanied by fragmentation of the C_{60}^+ molecular ion in the photon energy range 18–150 eV. Results for photofragmentation without ionization of C_{60}^+ are also reported in the 18–65 eV range. The current measurements for single photoionization of C_{60}^+ supersede those reported in reference [10] and extend the photon energy range up to 150 eV.

II. EXPERIMENT

The measurements were performed at the ion photon beam (IPB) endstation on undulator beamline 10.0.1 of the Advanced Light Source. The merged-beams setup and the general experimental method have been described at length [25, 26], and only a brief description with details unique to the present investigation are reported here.

C_{60}^+ ions were produced by evaporating high-purity commercial C_{60} powder from a small resistively heated oven into an Ar discharge within the plasma chamber of a permanent-magnet electron-cyclotron resonance ion source [27]. The RF power at 10 GHz was maintained as low as possible to minimize the collisional fragmentation of fullerenes in the ion source discharge prior to acceleration [10].

A 6–keV beam of C_{60}^+ ions was extracted from the ion source, focused, collimated and mass analyzed prior to being electrostatically merged onto the axis of a counter-propagating beam of monochromatized synchrotron radiation along a common path of approximately 1.4 m in ultra-high vacuum. The ion beam was subsequently de-merged from the photon beam by a dipole magnet. The magnet and a spherical electrostatic analyzer located immediately downstream deflected the product ion beam in

orthogonal directions and selectively directed products of a specific mass and charge state to a channeltron-based single-particle detector [28]. The detection efficiency for 6 keV C_{60}^{2+} was measured *in situ* to be 0.79±0.03. Four-jaw slits located in front of the detector permitted adjustment of the resolution of the spatially resolved mass/charge distribution of product ions. Spectroscopic scans were made for each product by recording the count rate as the photon beam energy was stepped over the range 18–150 eV in intervals of typically 0.5 eV. The photon beam was mechanically chopped at 6 Hz to separate photo-products from the same products produced by collisions with residual gas in the ultra-high vacuum system or by auto-fragmentation due to internal vibrational excitation in the parent C_{60}^+ ion beam. The primary ion beam was simultaneously collected in a Faraday cup and its current measured by a precision electrometer. The photon beam was directed onto a calibrated Si X-ray photodiode from which the photocurrent provided a measure of its absolute intensity.

For cross-section measurements at specific photon beam energies the spatial overlap of the beams in a central electrostatically biased interaction region of length 29.4 ± 0.6 cm was quantified using three translating-slit scanners located near the beginning, middle and end of their common interaction path. The bias potential facilitated energy labeling of products produced within that region where the spatial overlap of the two beams was accurately quantified. Simultaneously stepping the dipole magnetic field and spherical deflector voltage permitted a mapping of the different product ion masses and charge states under identical beam-overlap conditions. As an illustration, Fig. 1 presents the product-ion distribution recorded for a primary beam of C_{60}^+ irradiated at a fixed photon beam energy of 65 eV. Doubly-ionized fullerene products that have lost as many as five pairs of C atoms are evident. For the cross section measurements the deflector potential and the magnetic field were set to appropriate values to ensure full collection of the chosen heavy photo-product.

The measurements were carried out in a systematic manner in four stages. First, spectroscopic measurements were made by merging the photon and C_{60}^+ ion beams and recording the normalized yield of C_{60}^{2+} ions due to pure ionization as the photon beam energy was scanned in 0.5 eV steps over the energy range 18–150 eV. This required use of two monochromator gratings, the first spanning the 18–75 eV range and the second the 65–150 eV range, and subsequently joining the two normalized spectral scans together. Because the monochromator slits were fixed during these scans, the photon energy resolution varied across this energy range, but was everywhere comparable to or better than the energy step size, which was typically 0.1 eV. The photon energy resolution was considered unimportant because of the absence of narrow resonance features in the cross sections.

The second stage was to perform absolute cross-section measurements for single ionization yielding C_{60}^{2+} prod-
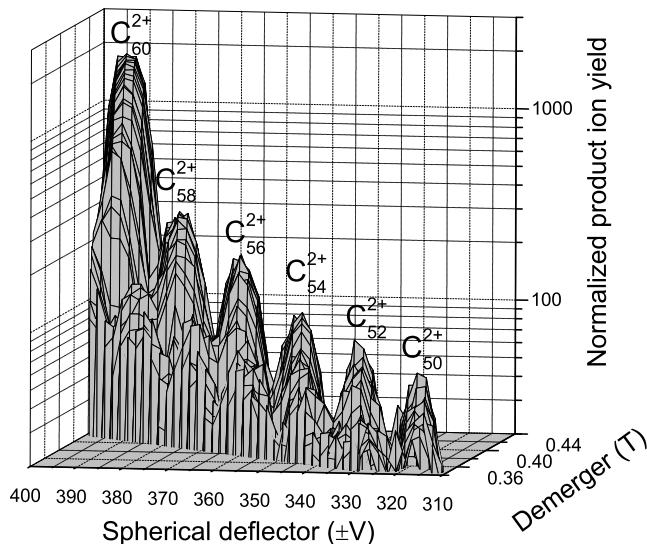
FIG. 1: Measured two-dimensional doubly charged product ion scans for a primary ion beam of C_{60}^+ irradiated at a fixed photon energy of 65 eV [24]. The demerging magnet and spherical electrostatic plates deflect the product ions across the detector in orthogonal directions [25], permitting scans of the product space following photoabsorption.

ucts under conditions in which the spatial overlap of the beams in the central interaction region was measured and well-characterized. These measurements were made at nine different photon energies distributed within the 18–150 eV energy range. The broad spectroscopic scan for the C_{60}^{2+} product ion was then placed on an absolute scale by normalizing it to these cross-section measurements.

The third stage involved measuring ratios of signal count rates for each of the other 22 ion products investigated to those for pure ionization yielding C_{60}^{2+} under identical beam-overlap conditions. These ratios were measured at as many as nine photon energies in the 18–150 eV range, permitting absolute cross sections to be determined for each product ion at those energies.

The fourth stage was to record spectroscopic photon-energy scans for each of the 22 ion products similar to that for C_{60}^{2+} and to use cross-section values obtained from the signal-ratio measurements to place the scans on an absolute scale. The results are collected and presented in graphical form in the following subsections. The absolute cross-section measurements performed at discrete photon energies and the cross-section values determined from signal ratios are tabulated in the Appendix. Their total systematic uncertainty is estimated to be ± 24%, except for the singly-ionized products from pure dissociation, for which it is estimated to be ± 30%. Statistical uncertainties are in all cases negligibly small in comparison.

III.   RESULTS

A.   Single ionization and single ionization with fragmentation

The ionization potential of C_{60}^+ is 11.35 eV [15, 29, 30], which is below the photon energy range accessible to the current experiment. The present absolute cross-section measurement for single photoionization of C_{60}^+ (without fragmentation) is compared with previously published data of Scully et al. [10] using the same apparatus in Fig. 2. While the two sets of data agree within the present absolute uncertainty of ± 24%, some differences in the measured energy dependences of the cross section are evident at photon energies below 20 eV and in the 30–40 eV range. These are attributed to four subsequent refinements in the experimental method. First, a photodiode that is more resistant to radiation damage improved the reliability of measurement of the absolute photon flux. Second, the effects of higher-order radiation from the synchrotron undulator were systematically evaluated [31] and appropriate corrections to the photodiode current and photoion signals were applied to the present data. Third, a likely reduction in the internal vibrational-rotational energy of the C_{60}^+ primary ion beam resulted from use of a 10–GHz traveling-wave-tube amplifier that made it possible to sustain a discharge in the ECR ion source at lower RF power (typically 1 W or less). Fourth, a photoion detector with adjustable four-jaw slits improved the product-ion resolution, insuring that C_{60}^{2+} and C_{58}^{2+} products were fully separated. It is noted that the second broad plasmon resonance identified by Scully et al. near 38 eV is more prominent in the present data, which may be a result of this improved product mass resolution. A comparison of the current absolute measurements for single ionization of C_{60}^+ and for single ionization accompanied by the loss of as many as 7 pairs of C atoms is presented in Fig. 3. With increasing loss of pairs of C atoms, a decrease in the peak cross section as well as a shift in the onsets to higher photon energies is evident. An analysis of the measured onset energies for loss of 2 to 7 pairs of C atoms is presented in Fig. 4. The energy required to remove a pair of C atoms does not depend on the total number of pairs removed. A linear least-squares analysis of these data gives an estimate of the mean energy required to remove a C-atom pair from C_{60}^+ to be 6.38 ± 0.19 eV, consistent with the range 6.0–6.5 eV for C_{60} reported by Yoo et al. [6] .

B.   Double ionization and double ionization with fragmentation

The measured cross section for double photoionization of C_{60}^+ is presented in Fig. 5. The inset shows a blow-up of the threshold energy region. A linear least-squares fit to the onset of the cross section in this region yields a double-ionization threshold energy for C_{60}^+ of 30.2 ± 2 eV.
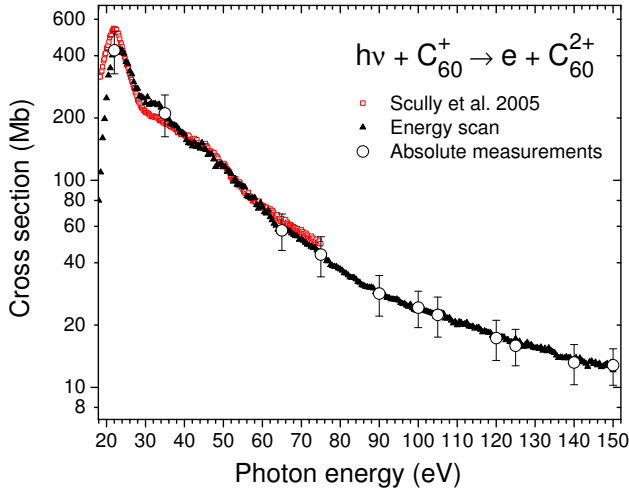
FIG. 2: Color online. Comparison of present results for single photoionization of C_{60}^{+} (solid triangles and open circles) with published results of Scully et al. (red open squares) [10].
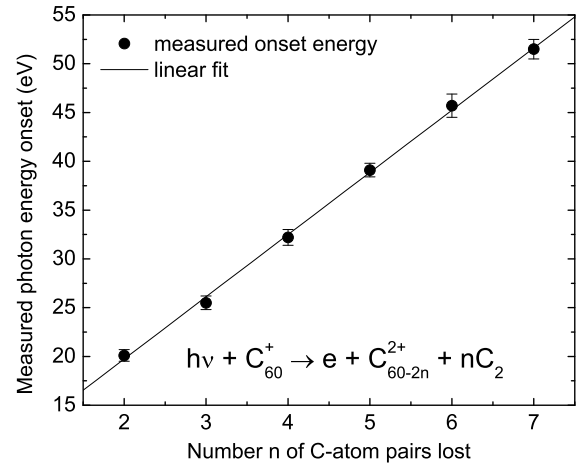
FIG. 4: Measured photon energy onsets for removal of 2 to 7 pairs of C atoms accompanying single ionization of C_{60}^{+}. The line represents a linear fit to the data.

The departure from linearity predicted by the Wannier threshold law [32] is so small that considering the statistical scatter in the data, it was considered insignificant compared to the fitting uncertainty. This result is consistent with the values of 32.15 ± 0.57 eV deduced from the measured onset energies for triple ionization of C_{60} reported by Juranić et al [15], 28.0 ± 1.5 eV by Wörgötter et al. [29] and 28.2 ± 0.5 eV by Pogulay et al. [30]. The small cross section below 30 eV with an onset near 23 eV may be due to production of C_{20}^{+} fragments from vibrationally excited primary C_{60}^{+} ions. This product has the same mass/charge ratio as C_{60}^{3+} and therefore could not be distinguished in the experiment. Figure 6 compares the measured cross sections for double photoionization of C_{60}^{+} accompanied by the loss of as many as seven pairs of C atoms. A linear-regression analysis of the cross-section onset energies as a function of the number of C-atom pairs lost similar to that in Fig. 4 for single photoionization with fragmentation gives a mean value of 7.02 ± 0.26 eV. This is slightly larger than the value of 6.38 ± 0.19 eV determined in the case of fragmentation accompanying single photoionization.

C.   Fragmentation of C_{60}^{+} without ionization

Additional cross-section measurements were made of fragmentation of C_{60}^{+} without ionization resulting in the loss of 2–8 pairs of C atoms over the photon energy range 18–65 eV. The results are presented in Fig. 7. It was not possible to experimentally resolve C_{58}^{+} products from the primary C_{60}^{+} ion beam which was more intense by roughly 6 orders of magnitude. These product channels for pure dissociation have cross sections that are larger than those for the corresponding product channels involving fragmentation with ionization and therefore account
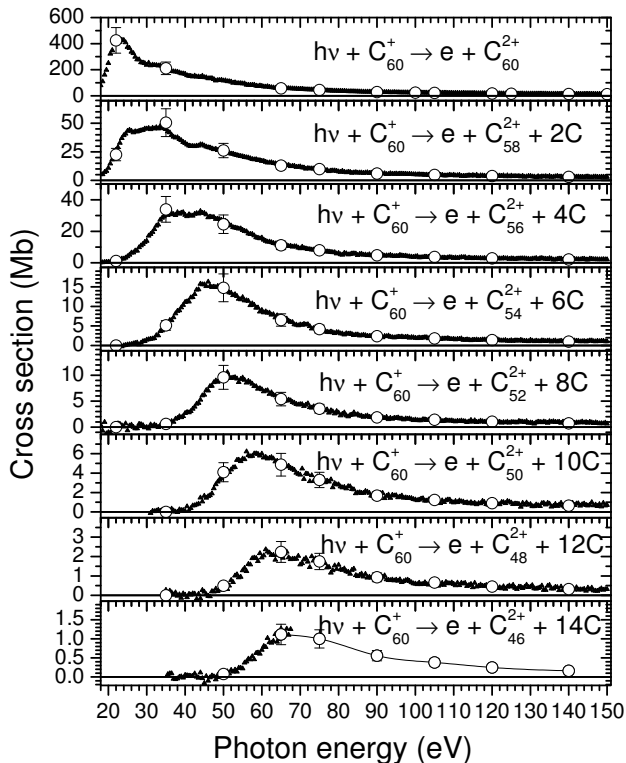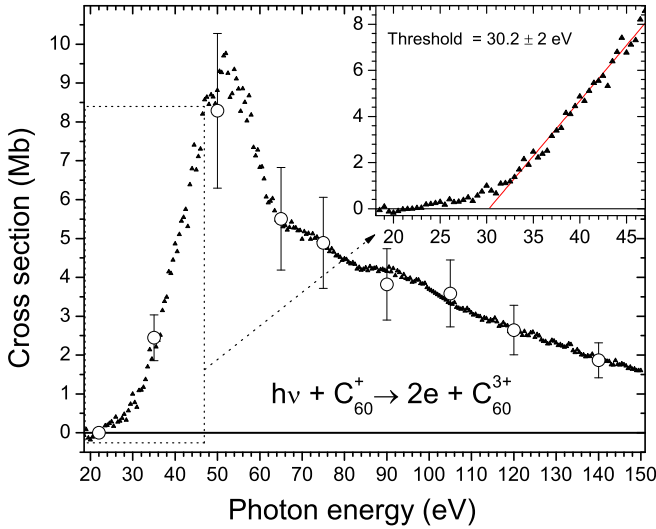

FIG. 3: Absolute measurements of cross sections for single photoionization of C_{60}^{+} and for single photoionization accompanied by the loss of up to 7 pairs of C atoms.

FIG. 5: Measured cross section for double photoionization of C_{60}^{+}. The triangles represent a fine energy scan and the open circles with error bars designate absolute cross-section measurements to which the scan has been normalized. The inset shows the threshold energy region on an expanded scale and a linear regression analysis to determine the double-ionization threshold energy.
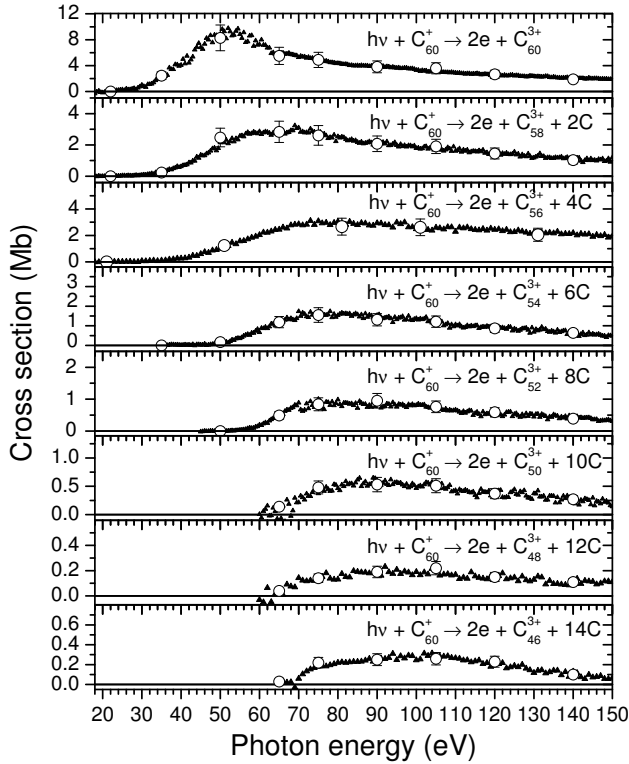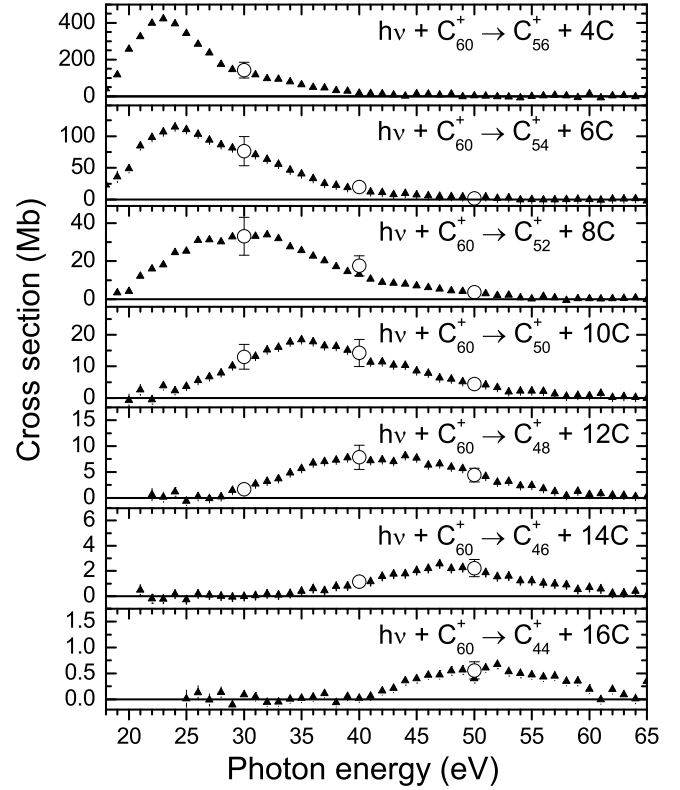

FIG. 7: Cross section measurements for fragmentation without ionization of C_{60}^{+} resulting in the loss of 2 to 8 pairs of C atoms. Open circles denote absolute cross sections determined from signal-ratio measurements.

for a significant fraction of the photoabsorption oscillator strength in the investigated range of photon energies. It should be noted that following the maxima, the cross sections for pure dissociation decrease much more rapidly with photon energy than those for the corresponding degree of fragmentation accompanied by ionization.

D. Total photoabsorption cross section and oscillator strength

An experimental estimate of the total photoabsorption cross section of C_{60}^{+} may be obtained by summing those for the 23 product ion channels that were investigated. Although the maximum photon energy for measurements of photofragmentation without ionization was only 65 eV, Fig. 7 shows that the cross sections have decreased essentially to zero at 65 eV for all the measured products. The result for C_{60}^{+} is shown in Fig. 8 and compared to a recent calculation of the total photoabsorption cross section of neutral C_{60} based on time-dependent density-functional theory (TDDFT) [33]. In this comparison it should be noted that the ionization potential of C_{60} is 7.65 eV compared to 11.55 eV for C_{60}^{+}. It should further be noted

FIG. 6: Measured absolute cross sections for double photoionization of C_{60}^{+} and for double photoionization accompanied by the loss of up to 7 pairs of C atoms.

that the C_{58}^+ product channel could not be measured in the present experiment and is missing from the sum, resulting in an underestimation of the total photoabsorption cross section of C_{60}^+. Given these considerations, the comparison is favorable, indicating the consistency of the experimental data and that the majority of important product channels resulting from photabsorption by C_{60}^+ were accounted for in the present experiment.

The near-absence of theoretically predicted structure in the present C_{60}^+ data is noteworthy because the photoabsorption cross sections for C_{60} and C_{60}^+ are expected to be similar, except at low energies because of their different ionization potentials. There is some evidence in the C_{60}^+ data in Fig. 8 for structure that was observed near 35 eV and 45 eV in the C_{60} data of Kafle et al. [8] but it is less pronounced. The photon energy resolution in the current experiment was sufficient to resolve any features similar to those predicted by the TDDFT calculation of Verhovtsev et al. [33] for C_{60}. Damping of structure in the measured cross section may be a manifestation of internal vibrational excitation of the parent C_{60}^+ ion beam produced by the ECR ion source. Thermal vibrational excitation is to be expected because solid C_{60} was evaporated in the experiments reported by Kafle et al. [8] at temperatures in the 703–770 K range and C_{60} was evaporated into the ion source in the present experiment at comparable temperatures. Because the C_{60}^+ ions are produced in an electrical discharge, additional vibrational excitation due to collisions within the ion source is possible and this may be responsible for reduced structure in the C_{60}^+ measurement compared to that for C_{60}.

An experimental estimate of the dimensionless oscillator strength may be determined by integrating the measured cross sections over an appropriate energy range as follows:

$$f = 9.11 \times 10^{-3} \int_{E_1}^{E_2} \sigma(E) dE \qquad (1)$$

where the photon energies E are in eV and the cross section σ is in Mb. Summing the cross sections for the measured product ion channels from a primary beam of C_{60}^+ and integrating between $E_1 = 18$ eV and $E_2 = 150$ eV yields a dimensionless oscillator strength of 147±35 for the channels involving ionization and 61±18 for the pure fragmentation channels. The measured total of 208±54 compares to a theoretical total photoabsorption oscillator strength based on the TRK sum rule of 239 corresponding to the number of L-shell electrons in the C_{60}^+ molecule. The 120 K-shell electrons are excluded because they are inaccessible by photoabsorption in the energy range of the present experiment. It is noted once again that the C_{58}^+ product channel, which is expected to be relatively important, is missing from the measured sum, resulting in an underestimation of the experimental total photoabsorption cross section and oscillator strength. While products of photoexcitation other than those detected in the present experiment are possible, the accounting of
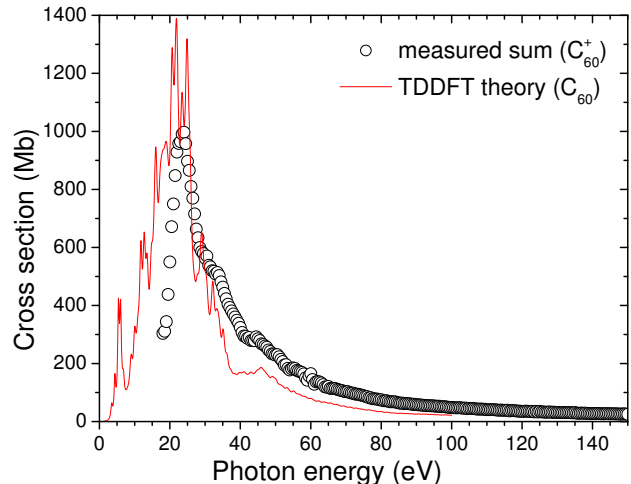

FIG. 8: Color online. Sum of the measured cross sections for all 23 product ion channels resulting from photoabsorption by C_{60}^+ ions (open circles) compared with the calculated photoabsorption cross section of neutral C_{60} from time-dependent density-functional theory (red curve) [33]. Note that the ionization potentials of C_{60} and C_{60}^+ are 7.65 eV and 11.35 eV, respectively.

oscillator strengths leads to the conclusion that the most important product channels were measured, with the exception of C58+, which likely accounts for the small remaining difference.

IV. SUMMARY AND CONCLUSIONS

Absolute cross sections were measured in the 18–150 eV range for single and double photoionization of C_{60}^+ accompanied by the loss of zero to seven pairs of C atoms. Threshold energies were determined for formation of the different product ion species when they occur within the measured energy range. Measurements were also made from 18–65 eV for fragmentation of C_{60}^+ unaccompanied by ionization resulting in the loss of 2-8 pairs of C atoms. Particularly noteworthy is the result that product channels involving (any form of) fragmentation of C_{60}^+ forming a smaller fullerene ion together account for nearly half of the total measured photoabsorption oscillator strength in this energy range.

Even if all products following photoabsorption were accounted for in the present experiment, the measured value of the total oscillator strength would be expected to be lower than the theoretical sum-rule value. The reason is that L-shell photoabsorption may occur - though with reduced probability - at photon energies below and above the range of the present measurements. One noteworthy consequence of the present total oscillator-strength measurement is that photoabsorption by C_{60}^+ in this en-

ergy range predominantly yields a product fullerene ion, nearly half the time consisting of a reduced number of C atoms.

The double-photoionization threshold energy for C_{60}^+ was determined from the measurements to be 30.2 ± 2 eV, which is consistent with values deduced from reported onset measurements of triple photoionization of C_{60} [15, 29, 30]. The average energies required for release of a pair of C atoms accompanying single and double photoionization of C_{60}^+ were determined to be 6.38 ± 0.19 eV and 7.02 ± 0.26 eV, respectively. These values compare with 6.0–6.5 eV reported by Yoo et al. [6] for photofragmentation of C_{60}^+ yielding C_{58}^+. Together these results suggest a possible dependence on the charge of the product fullerene ion.

Acknowledgments

[1] H. W. Kroto, J. R. Heath, S. C. O'Brien, R. F. Curl, and R. E. Smalley, Nature (London) **318**, 162 (1985).

[2] F. Lépine, J. Phys. B: At. Mol. Opt. Phys. **48**, 122002 (2015).

[3] I. V. Hertel, H. Steger, J. de Vries, B. Weissner, C. Menzel, B. Kamke, and W. Kamke, Phys. Rev. Lett. **68**, 784 (1992).

[4] G. F. Bertsch, A. Bulgac, D. Tománek, and Y. Wang, Phys. Rev. Lett. **67**, 2690 (1991).

[5] J. Berkowitz, J. Chem. Phys **111**, 1446 (1999).

[6] R. K. Yoo, B. Ruscic, and J. Berkowitz, J. Chem. Phys. **96**, 911 (1992).

[7] A. Reinköster, S. Korica, G. Prümper, J. Viefhaus, K. Godehusen, O. Schwarzkopf, M. Mast, and U. Becker, J. Phys. B **37**, 2135 (2004).

[8] B. P. Kafle, H. Katayanagi, M. S. I. Prodhan, H. Yagi, C. Huang, and K. Mitsuke, J. Phys. Soc. Japan **77**, 014302 (2008).

[9] S. Wang, Phys. Rev. A **60**, 262 (1999).

[10] S. W. J. Scully, E. D. Emmons, M. F. Gharaibeh, R. A. Phaneuf, A. L. D. Kilcoyne, A. S. Schlachter, S. Schippers, A. Müller, H. S. Chakraborty, M. E. Madjet, J. M. Rost, Phys. Rev. Lett. **94**, 065503 (2005).

[11] A. V. Korol and A. V. Solov'yov, Phys. Rev. Lett. **98**, 179601 (2007).

[12] S. W. J. Scully, E. D. Emmons, M. F. Gharaibeh, R. A. Phaneuf, A. L. D. Kilcoyne, A. S. Schlachter, S. Schippers, A. Müller, H. S. Chakraborty, M. E. Madjet, J. M. Rost, Phys. Rev. Lett. **98**, 179602 (2007).

[13] R. A. Phaneuf, in *Handbook of Nanophysics*, edited by K. D. Sattler (CRC Press, Taylor & Francis Group, 2011), vol. 2, pp. 35–1 – 35–11.

[14] S. C. O'Brien, J. R. Heath, R. F. Curl, and R. E. Smalley, J. Chem. Phys. **88**, 220 (1988).

[15] P. N. Juranić, D. Lukić, K. Barger, and R. Wehlitz, J. Phys. B: At. Mol. Opt. Phys. **73**, 042701 (2006).

[16] R. E. Stanton, J. Chem. Phys. **96**, 111 (1992).

[17] W. C. Eckhoff and G. E. Scuseria, Chem. Phys. Lett. **216**, 399 (1993).

[18] C. H. Xu and G. E. Scuseria, Phys. Rev. Lett. **72**, 669 (1994).

[19] A. D. Boese and G. E. Scuseria, Chem. Phys. Lett. **294**, 233 (1998).

[20] G. Sánchez, S. Diaz-Tendero, M. Alcami, and F. Martin, Chem. Phys. Lett. **416**, 14 (2005).

[21] H. Zettergren, G. Sánchez, and S. Diaz-Tendero, J. Chem. Phys. **127**, 104308 (2007).

[22] Y. H. Hu, Chem. Phys. Lett. **463**, 155 (2008).

[23] A. L. D. Kilcoyne, A. Aguilar, A. Müller, S. Schippers, C. Cisneros, G. Alna'Washi, N. B. Aryal, K. K. Baral, D. A. Esteves, C. M. Thomas, R. A. Phaneuf, Phys. Rev. Lett. **105**, 213001 (2010).

[24] R. A. Phaneuf, A. L. D. Kilcoyne, N. B. Aryal, K. K. Baral, D. A. Esteves-Macaluso, C. M. Thomas, J. Hellhund, R. Lomsadze, T. W. Gorczyca, C. P. Ballance, S. T. Manson, M. F. Hasoglu, S. Schippers, A. Müller, Phys. Rev. A **88**, 053402 (2013).

[25] A. M. Covington, A. Aguilar, I. R. Covington, M. F. Gharaibeh, G. Hinojosa, C. A. Shirley, R. A. Phaneuf, I. Álvarez, C. Cisneros, I. Dominguez-Lopez, M. M. Sant'Anna, A. S. Schlachter, B. M. McLaughlin, A. Dalgarno, Phys. Rev. A **66**, 062710 (2002).

[26] G. Alna'Washi, M. Lu, M. Habibi, R. A. Phaneuf, A. L. D. Kilcoyne, A. S. Schlachter, C. Cisneros, and B. M. McLaughlin, Phys. Rev. A **81**, 053416 (2010).

[27] F. Broetz, R. Trassl, R. W. McCullough, W. Arnold, and E. Salzborn, Phys. Scr. **92**, 278 (2001).

[28] K. Rinn, A. Müller, H. Eichenauer, and E. Salzborn, Phys. Sci. Instrum. **53**, 829 (1982).

[29] R. Wörgötter, B. Dünser, P. Scheier, and T. D. Märk, J. Chem. Phys. **101**, 8674 (1994).

[30] A. V. Pogulay, R. R. Abzalimov, S. K. Nasibullaev, A. S.

Lobach, T. Drewello, and Y. V. Vasilev, Int. J. Mass. Spectrom. **233**, 165 (2004).

[31] A. Müller, S. Schippers, J. Hellhund, K. Holste, A. L. D. Kilcoyne, R. A. Phaneuf, C. P. Ballance, and B. M. McLaughlin, J. Phys. B: At. Mol. Opt. Phys. **48**, 235203 (2015).

[32] R. Wehlitz, M. -T. Huang, I. A. Sellin, and Y. Azuma, J. Phys. B: At. Mol. Opt. Phys. **32**, L635 (1999).

[33] A. V. Verkhovtsev, A. V. Korol, and A. V. Solov'yov, Phys. Rev. A **88**, 043201 (2013).

Appendix: Tables of Measured Cross Sections

TABLE I: Measured absolute cross sections for single photoionization of C_{60}^+. Absolute uncertainties correspond to a one-sigma confidence level.

Photon Energy (eV)	Cross Section (Mb)	Absolute Uncertainty (Mb)
22	425	98
35	211	48
65	57.4	11.5
75	43.8	9.6
90	28.4	6.3
100	24.3	4.9
105	22.4	4.9
120	17.3	3.8
125	15.9	3.2
140	13.2	2.9
150	12.8	2.6

TABLE II: Cross sections determined from product signal ratios for single photoionization of C_{60}^+ with loss of $1 - 7$ pairs of C atoms. Absolute uncertainties are estimated to be $\pm 24\%$ at one-sigma confidence level.

Photon Energy (eV)	Product Ion						
	C_{58}^{2+} (Mb)	C_{56}^{2+} (Mb)	C_{54}^{2+} (Mb)	C_{52}^{2+} (Mb)	C_{50}^{2+} (Mb)	C_{48}^{2+} (Mb)	C_{46}^{2+} (Mb)
22	22.6	1.1	-	-	-	-	-
35	50.5	34.0	5.1	0.61	-	-	-
50	26.2	24.5	14.7	9.6	4.1	0.50	0.08
65	13.0	11.1	6.5	5.4	4.9	2.2	1.1
75	9.9	8.0	4.2	3.5	3.3	1.7	1.0
90	6.0	4.8	2.4	1.9	1.7	0.93	0.56
105	4.8	3.7	1.8	1.4	1.2	0.66	0.38
120	3.8	2.8	1.4	1.0	0.90	0.45	0.25
140	3.0	2.2	1.0	0.73	0.64	0.32	0.16

TABLE III: Cross sections determined from product signal ratios for double photoionization of C_{60}^+ with loss of $0 - 7$ pairs of C atoms. Absolute uncertainties are estimated to be $\pm 24\%$ at one-sigma confidence level.

Photon Energy (eV)	Product Ion							
	C_{60}^{3+} (Mb)	C_{58}^{3+} (Mb)	C_{56}^{3+} (Mb)	C_{54}^{3+} (Mb)	C_{52}^{3+} (Mb)	C_{50}^{3+} (Mb)	C_{48}^{3+} (Mb)	C_{46}^{3+} (Mb)
22	-	-	-	-	-	-	-	-
35	2.4	0.23	-	-	-	-	-	-
50	8.3	2.5	1.2	0.17	-	-	-	-
65	5.5	2.8	2.7	1.2	0.49	0.14	0.04	0.03
75	4.9	2.6	2.6	1.5	0.84	0.48	0.14	0.22
90	3.8	2.1	2.0	1.3	0.95	0.53	0.19	0.25
105	3.6	1.9	1.9	1.2	0.76	0.51	0.22	0.26
120	2.6	1.5	1.4	0.87	0.59	0.37	0.15	0.23
140	1.9	1.0	1.0	0.64	0.39	0.27	0.11	0.10

TABLE IV: Cross sections determined from product signal ratios for photofragmentation without ionization of C_{60}^+ resulting in loss of $2 - 7$ pairs of C atoms. Absolute uncertainties are estimated to be $\pm 30\%$ at one-sigma confidence level.

Photon Energy (eV)	Product Ion						
	C_{56}^+ (Mb)	C_{54}^+ (Mb)	C_{52}^{2+} (Mb)	C_{50}^+ (Mb)	C_{48}^+ (Mb)	C_{46}^+ (Mb)	C_{44}^+ (Mb)
30	142	77	33	13	1.6	-	-
40	-	20	18	14	7.8	1.1	-
50	-	2.0	3.6	4.4	4.4	2.2	0.56